

Calibrating Cross-modal Features for Text-Based Person Searching

Donglai Wei*
Fudan University
dlwei21@m.fudan.edu.cn

Sipeng Zhang
MEGVII Technology
zhangsipeng@megvii.com

Tong Yang
MEGVII Technology
yangtong@megvii.com

Yang Liu
Fudan University
yang.liu20@fudan.edu.cn

Jing Liu†
Fudan University
jingliu19@fudan.edu.cn

Abstract

*Text-Based Person Searching (TBPS) aims to identify the images of pedestrian targets from a large-scale gallery with given textual caption. For cross-modal TBPS task, it is critical to obtain well-distributed representation in the common embedding space to reduce the inter-modal gap. Furthermore, it is also essential to learn detailed image-text correspondence efficiently to discriminate similar targets and enable fine-grained target search. To address these challenges, we present a simple yet effective method that calibrates cross-modal features from these two perspectives. Our method consists of two novel losses to provide fine-grained cross-modal features. The **Sew** calibration loss takes the quality of textual captions as guidance and aligns features between image and text modalities. On the other hand, the **Masking Caption Modeling (MCM)** loss leverages a masked captions prediction task to establish detailed and generic relationships between textual and visual parts. The proposed method is cost-effective and can easily retrieve specific persons with textual captions. The architecture has only a dual-encoder without multi-level branches or extra interaction modules, making a high-speed inference. Our method achieves top results on three popular benchmarks with **73.81%**, **74.25%** and **57.35%** Rank1 accuracy on the **CUHK-PEDES**, **ICFG-PEDES**, and **RSTPReID**, respectively. We hope our scalable method will serve as a solid baseline and help ease future research in TBPS. The code will be publicly available.*

1. Introduction

Person re-identification (Re-ID) is a fundamental technology in the field of video surveillance [14, 25]. Its objec-

*This work is done during Donglai Wei’s internship at MEGVII Technology.

†Corresponding author.

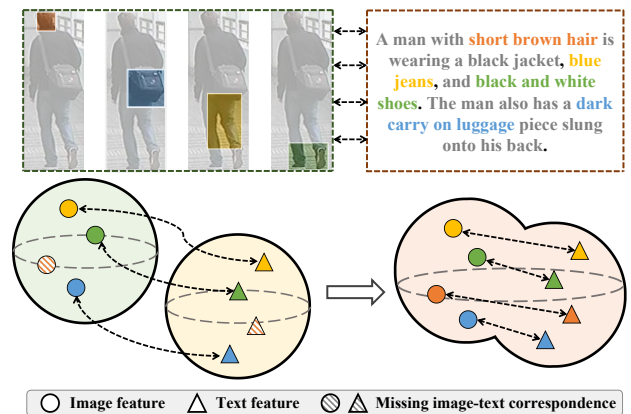


Figure 1. An illustration of our method’s motivation. For cross-modal tasks, a close and compact image-text feature distribution in the common embedding space is critical. Additionally, for the TBPS task, it is equally important to prevent missing the fine-grained image-text correspondence.

tive is to identify a target person from a large-scale image database using a query image. However, Re-ID has limitations in practical applications. For example, in criminal investigations, witnesses may provide only textual descriptions of the suspect without an accompanying image. To address this new scenario, Text-Based Person Searching (TBPS) [21] has recently gained increasing interest. TBPS allows retrieval of the target person solely based on textual captions as the query.

Compared to Re-ID, the main task of TBPS is to learn fine-grained cross-modal features between visual and textual modalities. As shown in Figure 1, cross-modal features have two key characteristics that contribute to searching a person from images: closely aligned cross-modal features and fine-grained information correspondence. First, closely aligned cross-modal features can reduce the inter-modal gap, making it easier to locate specific persons with

textual captions. Second, detailed correspondence is essential for TBPS. In some cases, fine-grained cross-modal information is necessary to discriminate between two similar persons.

In the TBPS task, there are numerous approaches proposed from two perspectives. First, some methods [1,42,44] employ only two encoders and align the two modal features using a symmetric loss. Although simple, the feature alignment is limited in their methods. The other methods [19,41] utilize multi-modal models with transformer-based [32] cross-attention to improve cross-modal feature alignment and interaction. However, such methods require the fusion of all possible image-text pairs, resulting in a time-consuming retrieval process during inference. Second, to obtain robust fine-grained features, recent TBPS works have designed multi-level [4, 8, 20, 35], multi-granularity [11,30,33] matching strategies, and specific attention modules [15, 21, 38]. These methods rely on the image-text backbone to provide fine-grained features. While these methods provide fine-grained features, they have complex model architectures and costly computations. Furthermore, the fine-grained features they produce are limited and hinder performance boost.

To address these issues, we propose a simple yet effective method for calibrating cross-modal features in TBPS. Our method consists of only a dual-encoder, making it simple and cost-effective without requiring complex interaction modules or extra multi-level branches, which allows for high-speed inference. In addition, we propose two novel training losses to calibrate cross-modal features. The first is a Sew calibration loss, which takes the quality of the text description as guidance and aligns features between the textual and visual modalities. It also pushes negative sample pairs apart and pulls positive sample pairs together across the two modalities. Next, we propose a Masking Caption Modeling (MCM) loss to obtain more fine-grained and generic correspondence. This loss uses a masked caption prediction task to establish detailed relationships between text parts and image parts. The operation is implemented through a cross-modal decoder that is discarded at the inference stage, avoiding extra computation cost.

To demonstrate the effectiveness of our method, we evaluated its performance on three popular benchmarks: CUHK-PEDES [21], ICFG-PEDES [8], and RSTPReID [45]. Our model surpasses the previous state-of-the-art methods and demonstrates impressive performance. Moreover, we conducted extensive experiments to validate each component of our method.

Overall, our major contributions can be summarised as follows:

- We introduce an effective and scalable framework to learn and calibrate cross-modal features for text-based person searching. Our framework utilizes a

dual-encoder and an auxiliary cross-modal decoder to achieve efficient and high-speed inference.

- We propose two novel losses, in which the Sew calibration loss aligns fine-grained features between image and text modalities, as well as the MCM loss establishes detailed relationships between vision modality and textual modality.
- Extensive experiments demonstrate the superiority of our framework. Our method achieves new state-of-the-art on three popular benchmarks: CUHK-PEDES, ICFG-PEDES, and RSTPReID, which reaches **73.81%**, **74.25%**, and **57.35%** on the Rank1, respectively.

2. Related Work

2.1. Text-Based Person Search

Text-based person searching is first introduced by [21], which identifies person images in a gallery only using a textual query. Early works utilized pre-task methods to obtain external cues such as person segmentation [35] and human body landmarks [22]. In recent years, end-to-end frameworks based on attention mechanisms [11, 15, 20, 21, 30, 38] have become prevailing. Cross-modal attention is critical for performing image-text interaction. Existing methods can be broadly classified into attention-explicit and attention-implicit. Specifically, attention-explicit methods [11, 15, 21, 38] design specific attention modules according to multi-granularity and multi-level strategies. For example, NAFS [11] conducts cross-modal alignments over full-scale features with a contextual non-local attention module. CFine [38] utilizes cross-attention for multi-grained global feature learning, it achieves impressive results on three benchmarks with knowledge transfer from the CLIP [27] model. In contrast attention-implicit methods [20, 30] utilize transformer-based models with shared parameters to align cross-modal semantics implicitly. SafaNet [20] introduces a semantic-aligned feature aggregation network. It utilizes a cross-modal parameter-sharing multi-head attention module following the backbone to enhance the extracted image-text representations. However, compared to performing in-depth cross attention with a task-driven approach, the existing methods do not implement enough cross-interaction with generalized performance.

2.2. Metric Learning

Initially, metric learning used L_2 distance as the metric, with the goal is to minimize the L_2 distance between samples of the same class. Some L_2 -based metric learning methods include Siamese Networks [3] and Triplet Networks [29]. With the development of deep learning, researchers started using softmax-based loss functions in met-

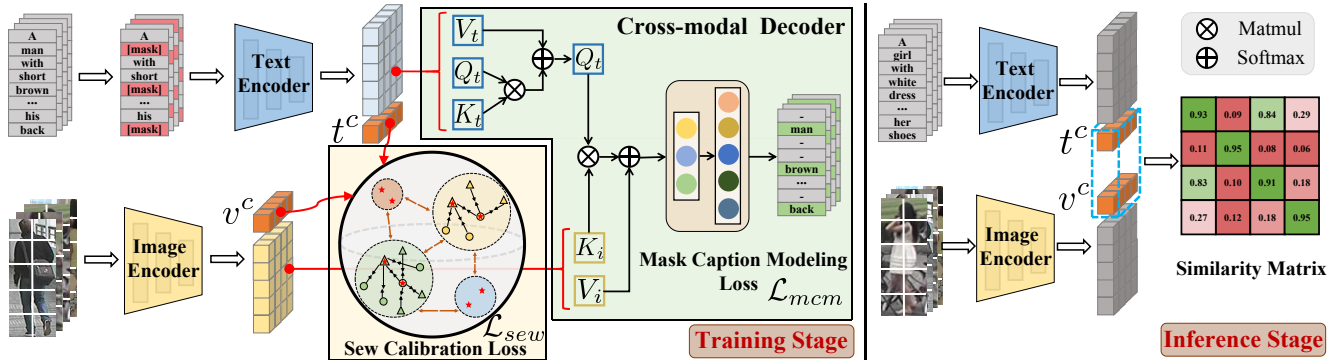


Figure 2. Overview of our proposed method. The framework consists of a dual-encoder for extracting image-text features and calibrating cross-modal features with the Sew Calibration loss. We also include a decoder for performing cross-modal interaction with the task-driven Mask Caption Modeling. At the inference stage, we only utilize the classification (CLS) tokens from the dual-encoder to implement similarity search.

ric learning to learn a more discriminative distance metric. Additionally, increasing the margin between classes is an intuitive approach to learn a better metric space. L-Softmax [24] introduced the concept of margin on softmax function for the first time. The widely used CosFace [34] proposed large-margin cosine loss to learn highly discriminative deep features for face recognition. Circle loss [31] proposed a simple loss based on a unified loss for metric learning and classification. Recently, some works introduced adaptive margin into marginal loss [17, 23, 26]. They usually learned image quality implicitly and adjust the margin accordingly. In single-modal representation learning, they usually give large margins to high-quality samples for hard mining. Compared to them, we try to solve a cross-modal matching problem where samples from two modalities have different information volume. We give greater tolerance to less informative samples in TBPS.

2.3. Masked Language Modeling

Masked Language Modeling (MLM) is a highly effective method for pre-training language models [6, 28] by randomly selecting a certain percentage of words from the input sentence and then predicting the masked words based on the context of other words. Many cross-modal pre-training models have utilized MLM in their methods [2, 18, 19]. For example, the work in [19] combines MLM with contrastive loss in the framework, which achieved impressive performance in their cross-modal tasks. The success of MLM in BERT [6] has proven its ability to adapt well to various downstream tasks, leading to generalized performance. In our fine-grained framework, the task-driven decoder utilizing masked caption modeling can facilitate generic cross-modal learning.

3. Methods

Formally, given a set of images with corresponding captions, denoted as $X = \{(I_i, T_i)\}_{i=1}^N$. Each image I_i and its description text T_i is associated with a person ID y_i . Text-based person search aims to retrieve the most relevant Rank k (e.g., $k = 1, 5, 10$) person images efficiently from a large-scale gallery with a textual caption. To solve this task, we propose a simple yet effective method, as shown in Figure 2.

We use ViT [9] and BERT [6] as the image-text encoders in our dual-encoder backbone. The image encoder takes image patches from I_i along with a vision classification (CLS) token as input. It outputs an image feature sequence v_i and a vision CLS token embedding v_i^c . Similarly, the text encoder obtains a text feature sequence t_i and a text CLS token embedding t_i^c for caption T_i , following previous works [11, 38].

3.1. Sew Calibration Loss with Constraints

In the TBPS task, closely aligning cross-modal features is crucial for effectively finding specific persons with textual captions. To address the heterogeneity between modalities, we propose a Sew calibration loss that pushes each modality to a common space.

As shown in Figure 3 (a), in single modality settings, a triplet distance constraint is widely utilized when embeddings are from a single modality distribution. In intra-class samples, the embeddings are pulled together, while inter-class samples are pushed away. In the cross-modal setting, we expect to impose constraints from both sides of the two embedding distributions. For example, in one-direction retrieval, we first need to align the features of a "perfect pair," i.e., (I_i, T_i) . The shortest distance from the image embedding v_i to the text embedding should be t_i . This is because it is a perfect matching pair in person re-identification, and no other text feature will have a shorter distance (Eq. 1). We set the perfect pair as an image-text

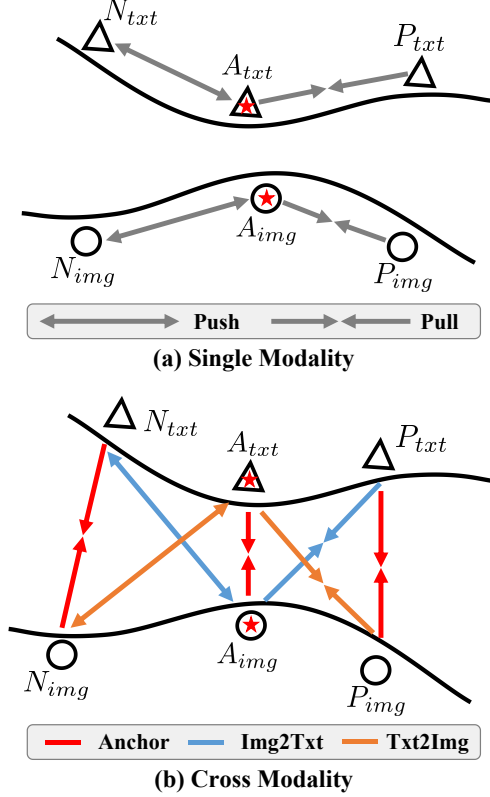


Figure 3. Illustration of Sew calibration loss. The constraints are different between single-modal and cross-modal matching. (A_{img}, A_{txt}) denotes anchors in image-text feature distribution, while (P_{img}, P_{txt}) and (N_{img}, N_{txt}) denote positive and negative sample pairs, respectively. The Sew calibration loss pushes negative sample pairs and pulls positive sample pairs, stitching cross-modal key information like a seam.

anchor (A_{img}, A_{txt}) . Next, we impose another constraint between the image anchor A_{img} and its corresponding positive text samples $P_{txt}(\mathbb{1}(y_i = y_j, i \neq j))$ and negative text samples N_{txt} (Eq. 2). For the other direction, we put symmetric constraints on A_{txt} and P_{img}, N_{img} . Figure 3 (b) shows the proposed constraints for cross modality. Forces from both sides act like a seam to pull the two distributions together.

Take the image side as an example, the L_2 distance constraints are shown as follows:

$$D(A_{img}, A_{txt}) + \mathcal{M}_1 < D(A_{img}, P_{txt}), \quad (1)$$

$$D(A_{img}, P_{txt}) + \mathcal{M}_2 < D(A_{img}, N_{txt}), \quad (2)$$

where D denotes L_2 distance. \mathcal{M}_1 and \mathcal{M}_2 are two margins, $\mathcal{M}_1 < \mathcal{M}_2$. With a bi-directional margin, each modal feature of the same pedestrian target is compressed compactly, making decision boundaries clearer.

We then relax the constraints to:

$$0.5D^2(A_{img}, A_{txt}) + \mathcal{M}_1 < 0.5D^2(A_{img}, P_{txt}), \quad (3)$$

$$0.5D^2(A_{img}, P_{txt}) + \mathcal{M}_2 < 0.5D^2(A_{img}, N_{txt}). \quad (4)$$

Subsequently, we change the above pairwise constraints into soft forms for better convergence following [31].

$$\mathcal{L}_{match}^{Pull} = \log\left[1 + \sum_{k=1}^K \exp(\alpha(\bar{v}_i^c \bar{t}_k^c - \bar{v}_i^c \bar{t}_i^c + \mathcal{M}_1))\right], \quad (5)$$

$$\mathcal{L}_{match}^{Push} = \log\left[1 + \sum_{k=1}^K \sum_{j=1}^J \exp(\alpha(\bar{v}_i^c \bar{t}_j^c - \bar{v}_i^c \bar{t}_k^c + \mathcal{M}_2))\right], \quad (6)$$

where \bar{v}^c and \bar{t}^c are CLS token features after normalizing, K and J denote the number of positive and negative samples in this batch, respectively. α is a scale parameter.

As a result, the image-to-text matching part of Sew calibration loss is formulated as below:

$$\mathcal{L}_{match}^{I2T} = \mathcal{L}_{match}^{Pull} + \mathcal{L}_{match}^{Push}. \quad (7)$$

The constraints in Eq. 2 can also be used to impose a classification loss in a similar way. As there is no difference for perfect positive samples in the classification task, we omit to constrain (1). Formally, the loss for our person ID classification part is as follows [42]:

$$\mathcal{L}_{id}^{I2T} = \frac{1}{n} \sum_{i=1}^n -\log\left(\frac{e^{\alpha(s_{y_i, i} - \mathcal{M}_2)}}{e^{\alpha(s_{y_i, i} - \mathcal{M}_2)} + \sum_{j \neq y_i} e^{\alpha(s_{y_j, i})}}\right), \quad (8)$$

$$s_{i, j} = \omega_i^T \hat{v}_j, \quad \hat{v}_i = (v_i^c)^T \bar{t}_i^c \cdot \bar{t}_i^c, \quad (9)$$

where n is batch size, and ω represents the classification weight after normalization. \hat{v}_i can be explained as the projection of image representation v_i^c onto the normalized text representation \bar{t}_i^c .

$\mathcal{L}_{match}^{T2I}$ and \mathcal{L}_{id}^{T2I} are in the same form as above, but the change is focused on the text-to-image. Both matching and classification loss have identical decision boundaries. Equipped with our proposed cross-modal constraints, the Sew calibration loss can reduce the gap between image and text feature distributions effectively.

Although the margin restrictions allow our model to learn better cross-modal features, using a fixed margin \mathcal{M} in all cases may not be flexible enough. A large margin constraint makes model learning difficult, while too small a margin does not impose a significant constraint. An adaptive margin guided by quality can be more effective. In TBPS, the texts come from the annotator's descriptions of the images. Images are expected to have complete information, while texts have varying amounts of information.

Thus, we adjust the margin value based on the quality of the text description. We argue that a less informative caption (i.e., a shorter caption) needs a smaller margin as a looser constraint. Based on this, we compute the adaptive margin for each image-text pair according to its text total tokens length \mathcal{T}_i :

$$\mathcal{M}_i = \mathcal{M}_{min} + \frac{(\mathcal{M}_{max} - \mathcal{M}_{min}) \cdot (\mathcal{T}_i - \mathcal{T}_{min})}{\mathcal{T}_{max} - \mathcal{T}_{min}}, \quad (10)$$

where \mathcal{M}_{max} and \mathcal{M}_{min} are upper and lower bounds of margins. \mathcal{T}_{max} and \mathcal{T}_{min} are bounds of the captions length, respectively. We set \mathcal{T}_{max} and \mathcal{T}_{min} according to the different dataset captions length distributions. After that, we utilize \mathcal{M}_i to replace the fixed margin \mathcal{M} above. We simply set $\mathcal{M}_1 = \mathcal{M}_2 = \mathcal{M}_i$. Compared to adaptive margins, we also report the detailed manual margin parameter analysis in the supplementary materials.

3.2. Masking Caption Modeling Loss

TBPS is a fine-grained cross-modal task, which means only caption-level discrimination is not enough. If the textual captions of two persons differ in a few words, a TBPS method can not retrieve a specific person without word-level discrimination. Although there are many works to establish word-level discrimination capacities, such methods are complex and limited, hindering performance boost. To solve this issue, we propose masking caption modeling to establish detailed image-text relationships. Furthermore, by utilizing MCM, our framework can perform more generic cross-modal learning.

Inspired by [7, 40], we add a masked prediction task on the text branch. Concretely, this loss is based on a cross-modal decoder architecture. We mask a portion of text tokens and replace these masked tokens with a learnable token vector. The text encoder inputs these text tokens and outputs the corresponding text features. The decoder learns to maximize the conditional likelihood of the masked text feature t_n under latent image feature sequence $\{v_i\}$ and text feature sequence $\{t_i\}$:

$$\mathcal{L}_{mcm} = - \sum_{n=1}^N \log P_{\theta}(t_n | \{t_i\}, \{v_i\}), \quad (11)$$

where N is the total masked token numbers in a caption.

As shown in Figure 2 cross-modal decoder part, the decoder takes both unmasked text tokens and masked tokens in their original order as input. The multi-head self-attention [32] first encodes the text features as Q_t, K_t, V_t , while the cross self-attention further improves the text features by taking into account the encoded image features as K_i, V_i for visual context. The final linear projection layer has the same number of output channels as the text vocabulary, and computes the cross entropy loss between the reconstructed and original words only on masked text tokens.

Algorithm 1: Pseudocode of the proposed framework

Input: Image I and text T ; A batch of n paired $\mathbb{G} = \{(I^1, T^1), (I^2, T^2), \dots, (I^n, T^n)\}$
Output: Training loss $(\mathcal{L}_{sew}, \mathcal{L}_{mcm})$ or (I_{cls}, T_{cls})

```

1 foreach  $T^i$  in set  $\mathbb{G}$  do
2   |  $T^i \leftarrow \text{mask}(T^i)$ ;
3 end
4 for  $i \leftarrow 1$  to  $\mathbb{G}$  do
5   |  $(I_{cls}^i, I_1^i, \dots, I_c^i) \leftarrow ViT(T^i)$ ;
6   |  $(T_{cls}^i, T_1^i, \dots, T_c^i) \leftarrow Bert(T^i)$ ;
7   | if Training Stage then
8     |  $(I_{cls}^i, T_{cls}^i) \leftarrow BatchNorm(I_{cls}^i, T_{cls}^i)$ ;
9     |  $I_{context}^i, T_{context}^i \leftarrow$ 
10    |  $(I_1^i, \dots, I_c^i), (T_1^i, \dots, T_c^i)$ ;
11    |  $T_{context}^i \leftarrow Attn(T_{context}^i)$ ;
12    |  $T_{cross}^i \leftarrow CrossAttn(T_{context}^i, I_{context}^i)$ ;
13    |  $\mathcal{L}_{sew}^i \leftarrow SewCalibration(I_{cls}^i, T_{cls}^i)$ ;
14    |  $\mathcal{L}_{mcm}^i \leftarrow MCM(T_{cross}^i, T^i)$ ;
15  | else
16  |  $\{(I_{cls}^1, T_{cls}^1), (I_{cls}^2, T_{cls}^2), \dots, (I_{cls}^i, T_{cls}^i)\} \leftarrow$ 
17  |  $(I_{cls}, T_{cls})$ ;
18 end
19 if Training Stage then
20 | return  $(\mathcal{L}_{sew}, \mathcal{L}_{mcm})$ ;
21 else
22 | return  $(I_{cls}, T_{cls})$ ;

```

It should be noted that the cross-modal decoder is only used during training and not during inference.

3.3. Total Loss

The total loss \mathcal{L} we optimized in each iteration is as follows:

$$\mathcal{L}_{sew} = \mathcal{L}_{match}^{I2T} + \mathcal{L}_{match}^{T2I} + \mathcal{L}_{id}^{I2T} + \mathcal{L}_{id}^{T2I},$$

$$\mathcal{L} = \lambda_1 \mathcal{L}_{sew} + \lambda_2 \mathcal{L}_{mcm}, \quad (12)$$

where λ_1 and λ_2 are hyperparameters to balance the different loss terms during training. The pseudocode of our framework pipeline is shown in Algorithm 1.

4. Experiments

4.1. Datasets and Evaluation Metric

We evaluate our method on three benchmarks: CUHK-PEDES [21], ICFG-PEDES [8], and RSTPReid [45].

CUHK-PEDES is the first large-scale benchmark for text-based person search tasks. This dataset contains 40,206 images of 13,003 person IDs collected from five person re-identification datasets. Each image has two different textual captions with an extensive vocabulary, and the average sentence length is 23.5. The testing set comprises 3,074 images and 6,148 descriptions of 1,000 persons. ICFG-PEDES contains 54,522 images of 4,102 persons. For each image, the corresponding description has an average length of 37 words. The testing set consists of 19,848 image-text pairs of 1,000 persons. RSTPReID contains 20,505 images of 4,101 persons, with each pedestrian having five images. It is divided into a training set with 3,701 persons, a validation set with 200 persons, and a testing set with 200 persons. For our evaluation metric, we report the Rank k ($k=1, 5, 10$) text-to-image accuracy, which is commonly used in previous works to evaluate text-based person search. Given a textual description as the query, if the top- k retrieved images contain any person corresponding to the query, we consider it a successful person search.

4.2. Implementation Details

In our visual-textual dual-encoder, we extract visual representations using the ViT-Base pre-trained on ImageNet [5]. The images are resized to 224×224 pixels. For textual representations, we use the BERT-Base-Uncased model pre-trained on the Toronto Book Corpus and Wikipedia. The representation dimension is set to 768, and the feature sequence lengths are set to 197 and 100, respectively.

During the training phase, we use a batch size of 64 and train for 60 epochs. We use Adam optimizer with an initial learning rate of 0.001. To augment our data, we apply a random horizontal flipping operation, and we use a mask ratio of 0.1 for randomly masking text tokens. The minimum and maximum textual information length boundaries \mathcal{T}_{min} and \mathcal{T}_{max} are set to 20-60, 25-65, and 22-60 according to the caption length distributions of CUHK-PEDES, ICFG-PEDES, and RSTPReID, respectively. The bounds of the upper and lower margin \mathcal{M} are set to 0.4 and 0.6, and the scale parameter α is set to 32. For each loss in the total loss function, the balance factors λ_1 and λ_2 are set equal to 1.

During the testing phase, we apply a re-ranking post-processing approach to improve search performance following NAFS [11]. We conduct the experiments on four NVIDIA 2080Ti GPUs using PyTorch.

4.3. Comparison with State-of-the-art Methods

Results on CUHK-PEDES. Table 1 compares our framework and previous methods on CUHK-PEDES. It can be observed that our method can outperform all previous methods by a large margin. Compared to the state-of-the-art work CFine [38], our method achieves 67.71%(+2.64%), 84.57%(+1.56%) and 89.44%(+0.44%) on Rank1, Rank5

Table 1. Comparison with state-of-the-art methods on the CUHK-PEDES dataset. Rank1, Rank5, and Rank10 accuracies (%) are reported. The bold number represents the best score. R denotes the re-ranking post-processing operations. C denotes the image encoder pre-trained on the CLIP model.

Method	Pub.	Rank1	Rank5	Rank10
GNA-RNN [21]	CVPR 17	19.05	-	53.64
Dual-path [44]	TOMM 20	44.40	66.26	75.07
CMPM/C [42]	ECCV 18	49.37	-	79.27
ViTAA [35]	ECCV 20	55.97	75.84	83.52
CMAAM [1]	WACV 20	56.68	77.18	84.86
VP Net [22]	TNNLS 22	58.83	81.25	86.72
HGA Net [43]	MM 20	59.00	79.49	86.62
SUM [36]	KBS 22	59.22	80.35	87.60
NAFS [11]	arXiv 21	59.94	79.86	86.70
NAFS+R [11]	arXiv 21	61.50	81.19	87.51
DSSL [45]	MM 21	59.98	80.41	87.56
DSSL+R [45]	MM 21	62.33	82.11	88.01
MGEL [33]	IJCAI 21	60.27	80.01	86.74
SSAN [8]	arXiv 21	61.37	80.15	86.73
ACSA [15]	TMM 22	63.56	81.40	87.70
ACSA+R [15]	TMM 22	68.67	85.61	90.66
ISANet [39]	arXiv 22	63.92	82.15	87.69
IVT [9]	ECCVW 22	64.00	82.72	88.95
TestReID [12]	BMVC 21	64.08	81.73	88.19
TestReID+R [12]	BMVC 21	64.40	81.27	87.96
SAFA Net [20]	ICASSP 22	64.13	82.62	88.40
TIPCB [4]	Neuro 22	64.26	83.19	89.10
CAIBC [37]	MM 22	64.43	82.87	88.37
AXM Net [10]	AAAI 22	64.44	80.52	86.77
CFine [38]	arXiv 22	65.07	83.01	89.00
CFine+C [38]	arXiv 22	69.57	85.93	91.15
Ours	-	67.71	84.57	89.44
Ours+R	-	71.09	86.78	91.23
Ours+C	-	69.61	86.01	90.90
Ours+R+C	-	73.81	88.89	92.77

and Rank10 without re-ranking. The state-of-the-art results on the CUHK-PEDES show the effectiveness of our method. With the help of re-ranking, our method shows an incremental boost to get a 71.09% Rank1 score. Furthermore, with a better image encoder pre-training on CLIP, our method achieves 73.81%, 88.89% , and 92.77% on three metrics, respectively. These consistent improvements show the scalability of our method across better pre-trained models and extra post-processing operations.

Results on ICFG-PEDES and RSTPReid. We also utilized other benchmarks to validate our method’s performance and generalization. The ICFG-PEDES and RSTPReid datasets are more challenging compared to CUHK-PEDES, and our method significantly outperformed

Table 2. Quantitative results on the ICFG-PEDES dataset.

Method	Pub.	Rank1	Rank5	Rank10
Dual-path [44]	TOMM 20	38.99	59.44	68.41
CMPM/C [42]	ECCV 18	43.51	65.44	74.26
ViTAA [35]	ECCV 20	50.98	68.79	75.78
SSAN [8]	arXiv 21	54.23	72.63	79.53
TIPCB [4]	Neuro 22	54.96	74.72	81.89
IVT [30]	ECCVW 22	56.04	73.60	80.22
ISANet [39]	arXiv 22	57.73	75.42	81.72
CFine [38]	arXiv 22	55.69	72.72	79.46
CFine+C [38]	arXiv 22	60.83	76.55	82.42
Ours	-	60.20	75.97	81.78
Ours+R	-	72.17	85.74	89.67
Ours+C	-	62.29	77.15	82.52
Ours+R+C	-	74.25	86.95	90.70

all state-of-the-art methods on these two datasets by a large margin, as reported in Tables 2 and 3. Compared with the state-of-the-art results [38] on ICFG-PEDES, our method achieved significant improvements, with scores of 60.20%(+4.51%), 75.97%(+3.25%), and 81.78%(+2.32%) on Rank1, Rank5, and Rank10, respectively. On the RSTPReid dataset, we achieved scores of 50.75% (+4.90%), 74.20%(+3.90%), and 81.70%(+3.30%) on the three metrics. With re-ranking post-processing, we were able to achieve scores of 72.17% and 55.35% on Rank1 for the two benchmarks, respectively.

We note that re-ranking also brings a significant boost, as our model learns clear and compact cross-modal key information patterns, and re-ranking can retrieve the correct feature neighbors more effectively. Moreover, by utilizing the CLIP pre-trained image model as an encoder, we achieved even better results, with scores of 74.25%, 86.95%, and 90.70% on ICFG-PEDES, and scores of 57.35%, 77.50%, and 85.50% on RSTPReid. These two challenging benchmark results demonstrate the robustness and scalability of our method.

4.4. Ablation Studies

4.4.1 Analysis of Model Components

To fully validate the performance of the different components in our method, we demonstrate the contributions of each part on CUHK-PEDES, as shown in Table 4. **Model 1** and **Model 2** show the results using ResNet [13] and ViT [9] as the image encoder, respectively, without the Sew Calibration and MCM losses. We utilize Model 2 as our baseline, and CMPM and CMPC [42] are used as loss functions in the baseline experiment. First, we compare ResNet-50 and ViT-Base as the image encoder and observe a performance improvement of 1.90%, 1.03%, and 0.69% on Rank1, Rank5,

Table 3. Quantitative results on the RSTPReid dataset.

Method	Pub.	Rank1	Rank5	Rank10
DSSL [45]	MM 21	32.43	55.08	63.19
SUM [36]	KBS 22	41.38	67.48	76.48
SSAN [8]	arXiv 21	43.50	67.80	77.15
IVT [30]	ECCVW 22	46.70	70.00	78.80
ACSA [15]	TMM 22	48.40	71.85	81.45
CFine [38]	arXiv 22	45.85	70.30	78.40
CFine+C [38]	arXiv 22	50.55	72.50	81.60
Ours	-	50.75	74.20	81.70
Ours+R	-	55.35	77.30	84.25
Ours+C	-	51.95	73.50	82.45
Ours+R+C	-	57.35	77.50	85.50

and Rank10, respectively. Based on this, we adopt ViT as the image encoder in the following experiments. We then validate the Sew calibration and MCM losses compared to the baseline. From **Models 2-4**, we observe that Sew calibration loss brings marginal improvement, and a common distribution can provide a better basis for optimizing the embedding space for fine-grained cross-modal recognition. Moreover, **Model 3** represents the Sew calibration loss with the fixed margin 0.5, while **Model 4** represents the Sew calibration loss with adaptive margins. We observe that **Model 4** achieves better results than a fixed manual margin, no matter how we tune the margin value, which demonstrates the effectiveness of adaptive constraints. We also find that MCM gives another substantial improvement to the baseline from **Model 2** to **Model 5**, indicating that the text-image detail mining capability is critical. Notably, when the two components are used jointly in **Model 6**, our method continues to improve and outperform the baseline by 4.57%, 2.99%, and 2.37% on the three metrics, respectively. This demonstrates that obtaining well-distributed image-text features in the common embedding space is essential for reducing the cross-modal gap. The consistent improvement in each component of the method demonstrates our effectiveness.

4.4.2 Impact of Sew Calibration Loss for Reducing Cross-modal Gap

Benefiting from the Sew calibration loss, which reduces the cross-modal gap, the learned representation distributions are closer than with the basic loss. To demonstrate this, we illustrate a comparison of singular value decomposition on cross-modal features, inspired by [16]. Specifically, Figure 4 (a) and (c) present the baseline and our method’s singular value decomposition for the text and image modalities. We computed the distance between these two modalities at specific singular values and reflected them in Fig-

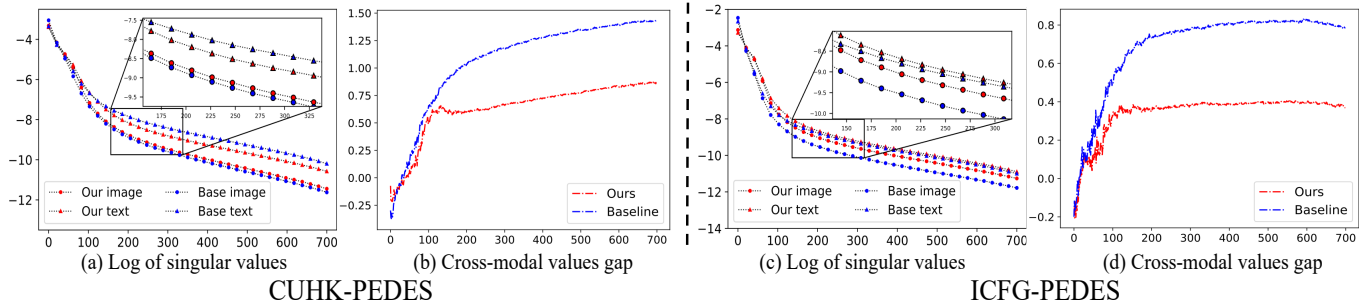


Figure 4. Comparison of different singular values of image-text embedding features on CUHK-PEDES (a) and ICFG-PEDES (c). A smaller gap between lines of the same type means their cross-modal distributions are closer. In (b) and (d), we show the specific log of singular values gap between baseline and our method.

Table 4. Performance comparisons of different components. **Res** and **ViT** denote ResNet and Vision Transformer for image encoder, respectively. **Sew-F** refers to the fixed margin Sew calibration loss, and **Sew-A** is the Sew calibration loss with adaptive margins. We utilize **Model 2** as our **baseline**.

ID	Res	ViT	Sew-F	Sew-A	MCM	Rank1	Rank5	Rank10
1	✓					60.39	80.22	86.53
2		✓				62.29	81.25	87.22
3		✓	✓			65.41	82.56	88.01
4		✓		✓		66.02	83.33	88.61
5		✓			✓	65.16	81.95	87.93
6		✓		✓	✓	67.71	84.57	89.44

Table 5. Ablation study of different masking caption modeling components on the CUHK-PEDES.

Mask	Attention	Caption Modeling	Rank1	Rank5	Rank10
✓			63.65	81.84	87.51
	✓		63.83	80.87	86.35
✓		✓	64.28	81.97	87.75
✓	✓	✓	65.16	81.95	87.93

ure 4 (b) and (d). Intuitively, the smaller the distance between different modality features, the closer the distribution learned by the model. We find that the Sew calibration loss performs better representation distributions in the common embedding space. It ensures closer cross-modal representation distributions and a smaller inter-modal gap than the baseline.

4.4.3 Impact of Masking Caption Modeling

The masking caption modeling operation in fine-grained cross-modal interaction is critical in our framework. It comprises tokens masking, attention module, and masked tokens prediction. As shown in Table 5, we explore the effec-

tiveness of MCM components on the CUHK-PEDES. First, only masking on the input text tokens without a reconstruction task behaves like a random erase text augmentation. This augmentation can already bring +1.36% marginal improvement and reach 63.65% on Rank1. It shows that the details provided by word tokens are helpful for fine-grained recognition.

Next, if we only utilize attention mechanism to enhance cross-modal representations without the mask caption modeling, it can achieve 63.83% on Rank1. We explain this improvement as the cross-attention brings details from sequence tokens to the CLS token. Meanwhile, image features also contribute a lot to this process.

On the other hand, we also design experiment of mask caption modeling without the cross attention. The decoder directly predicts all masked tokens from dual-encoder outputs. In this experiment, we observe 64.28% on Rank1. It proves the reconstruction tasks in decoder help guide the text encoder to learn richer and more refined representations. We also notice that with all three components, the MCM achieves 65.16% on Rank1. With the help of cross attention from image features, the CLS token ensembles all those rich information.

4.4.4 Analysis of Generalisability Validation

To better understand the contributions of MCM in our framework, we conduct a domain generalization analysis on the three benchmarks to demonstrate our generalization performance. In Table 6, CUHK \Rightarrow ICFG and CUHK \Rightarrow RSTP indicate using the model trained on the CUHK-PEDES dataset to infer their test sets and vice versa. Compared to the baseline, we can observe a performance improvement in the three metrics for ICFG-PEDES and RSTPReid. The fine-grained features mined by MCM are more resistant to overfitting. The improvement in domain generalization shows the capability of our framework in learning generic cross-modal information, which is essential to solve

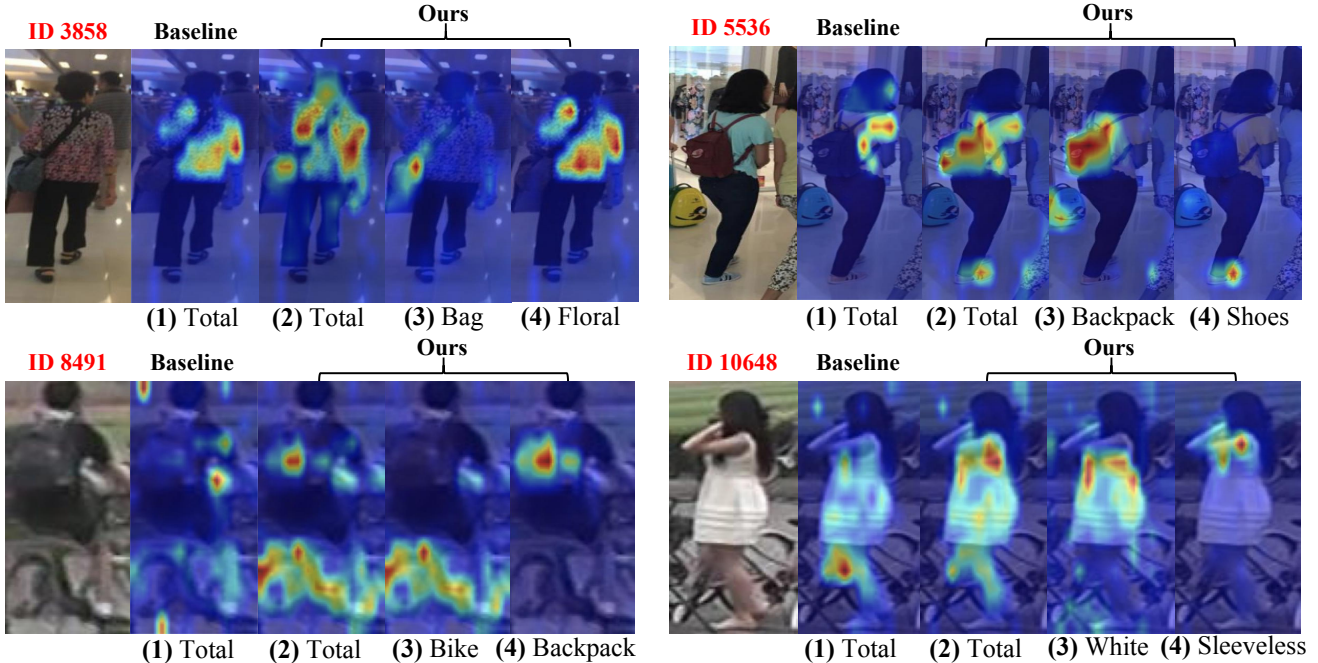


Figure 5. Visualization of attention maps from baseline and our method on the CUHK-PEDES. We present the total caption-level results and the fine-grained word-level results, respectively. (1) Baseline caption-level results, (2) Our caption-level results, (3) & (4) Our word-level results. Best viewed in color.

Table 6. Generic performance analysis on the three benchmarks for cross-domain validation.

CUHK \Rightarrow ICFG	Rank1	Rank5	Rank10
Baseline	30.79	49.10	57.47
Baseline+MCM	31.13	49.52	58.07
ICFG \Rightarrow CUHK	Rank1	Rank5	Rank10
Baseline	22.19	40.55	50.52
Baseline+MCM	23.78	42.41	52.11
CUHK \Rightarrow RSTP	Rank1	Rank5	Rank10
Baseline	37.40	63.40	74.35
Baseline+MCM	39.25	63.95	74.55
RSTP \Rightarrow CUHK	Rank1	Rank5	Rank10
Baseline	10.02	22.95	31.04
Baseline+MCM	10.69	25.20	33.93

the fine-grained modal heterogeneity.

4.5. Qualitative Analysis

4.5.1 Visualization of Attention Map

We visualize attention maps on the CUHK-PEDES test dataset to demonstrate model capability in learning image-text correspondence. In Figure 5, compared to the baseline, we can observe that the visualization results obtained by our method are more apparent and refined. We conduct the

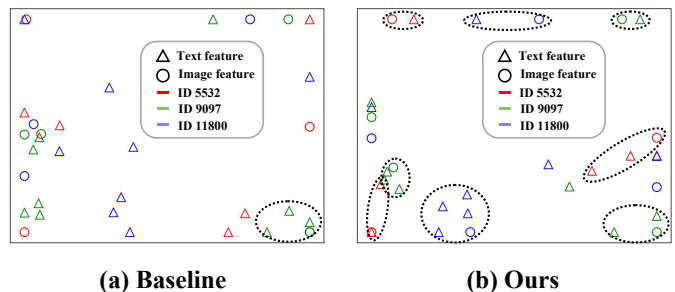


Figure 6. Presentation of cross-modal representation distributions on CUHK-PEDES test dataset. Different colors correspond to the different target ID. Best viewed in color.

word-level visualization to validate further the ability to perform fine-grained interaction. We select several keywords in the caption description, e.g., bag, shoes as items, colors, and clothing as modifiers. For example, the visualization results of IDs 8491 and 10648 do not focus on useful detailed information. The key messages in the two images are a man riding bike with a backpack and a woman wearing a sleeveless white dress. We can observe that our method successfully captures the key detail information compared to the baseline. From the word-level results, we can also observe that our method learns the critical parts in the cross-modal correspondence.

4.5.2 Visualization of Image-text Feature Distribution

Our method is capable of learning better image-text representation distributions with fine-grained image-text interaction and adaptive constraints to reduce the cross-modal gap. To demonstrate this, we randomly selected some pedestrians and extracted their image-text global features, then mapped them to two dimensions for visualization in Figure 6 (a) and (b). For instance, we can take IDs 5532 and 11800 as examples. We can observe that the image-text features of the same ID distribution are compressed more compactly, and the boundaries between them are more apparent than the baseline results. This demonstrates the effectiveness of our method in mitigating the cross-modal gap.

5. Conclusion

In this work, we propose a simple yet effective method calibrating cross-modal features for text-based person searching. With a dual-encoder, our framework is simple and cost-effective without any extra multi-level branches or complex interaction modules. Our model makes a high-speed inference only based on the dual-encoder. Two novel losses are proposed in our method: Sew calibration and MCM losses. The Sew calibration loss aligns fine-grained features between vision and textual modalities, while the MCM loss establishes detailed relationships between textual and visual parts. In addition, the performance on the three popular benchmarks demonstrates the effectiveness and superiority of our method. We hope our effective framework will serve as a solid baseline for text-based person searching in the future.

References

- [1] Surbhi Aggarwal, Venkatesh Babu Radhakrishnan, and Anirban Chakraborty. Text-based person search via attribute-aided matching. In *Proceedings of the IEEE/CVF Winter Conference on Applications of Computer Vision (WACV)*, pages 2617–2625, 2020. 2, 6
- [2] Hangbo Bao, Wenhui Wang, Li Dong, Qiang Liu, Owais Khan Mohammed, Kriti Aggarwal, Subhojit Som, and Furu Wei. Vlmo: Unified vision-language pre-training with mixture-of-modality-experts. *arXiv preprint arXiv:2111.02358*, 2021. 3
- [3] Jane Bromley, Isabelle Guyon, Yann LeCun, Eduard Säckinger, and Roopak Shah. Signature verification using a” siamese” time delay neural network. *Advances in Neural Information Processing Systems*, 6, 1993. 2
- [4] Yuhao Chen, Guoqing Zhang, Yujiang Lu, Zhenxing Wang, and Yuhui Zheng. Tipcb: A simple but effective part-based convolutional baseline for text-based person search. *Neurocomputing*, 494:171–181, 2022. 2, 6, 7
- [5] Jia Deng, Wei Dong, Richard Socher, Li-Jia Li, Kai Li, and Li Fei-Fei. Imagenet: A large-scale hierarchical image database. In *2009 IEEE Conference on Computer Vision and Pattern Recognition (CVPR)*, pages 248–255. IEEE, 2009. 6
- [6] Jacob Devlin, Ming-Wei Chang, Kenton Lee, and Kristina Toutanova. Bert: Pre-training of deep bidirectional transformers for language understanding. *arXiv preprint arXiv:1810.04805*, 2018. 3
- [7] Jacob Devlin, Ming-Wei Chang, Kenton Lee, and Kristina Toutanova. Bert: Pre-training of deep bidirectional transformers for language understanding. *arXiv preprint arXiv:1810.04805*, 2018. 5
- [8] Zefeng Ding, Changxing Ding, Zhiyin Shao, and Dacheng Tao. Semantically self-aligned network for text-to-image part-aware person re-identification. *arXiv preprint arXiv:2107.12666*, 2021. 2, 5, 6, 7
- [9] Alexey Dosovitskiy, Lucas Beyer, Alexander Kolesnikov, Dirk Weissenborn, Xiaohua Zhai, Thomas Unterthiner, Mostafa Dehghani, Matthias Minderer, Georg Heigold, Sylvain Gelly, et al. An image is worth 16x16 words: Transformers for image recognition at scale. *arXiv preprint arXiv:2010.11929*, 2020. 3, 6, 7
- [10] Ammarah Farooq, Muhammad Awais, Josef Kittler, and Syed Safwan Khalid. Axm-net: cross-modal context sharing attention network for person re-id. *arXiv preprint arXiv:2101.08238*, 2021. 6
- [11] Chenyang Gao, Guanyu Cai, Xinyang Jiang, Feng Zheng, Jun Zhang, Yifei Gong, Pai Peng, Xiaowei Guo, and Xing Sun. Contextual non-local alignment over full-scale representation for text-based person search. *arXiv preprint arXiv:2101.03036*, 2021. 2, 3, 6
- [12] Xiao Han, Sen He, Li Zhang, and Tao Xiang. Text-based person search with limited data. *arXiv preprint arXiv:2110.10807*, 2021. 6
- [13] Kaiming He, Xiangyu Zhang, Shaoqing Ren, and Jian Sun. Deep residual learning for image recognition. In *Proceedings of the IEEE Conference on Computer Vision and Pattern Recognition (CVPR)*, pages 770–778, 2016. 7
- [14] Shuting He, Hao Luo, Pichao Wang, Fan Wang, Hao Li, and Wei Jiang. Transreid: Transformer-based object re-identification. In *Proceedings of the IEEE/CVF International Conference on Computer Vision*, pages 15013–15022, 2021. 1
- [15] Zhong Ji, Junhua Hu, Deyin Liu, Lin Yuanbo Wu, and Ye Zhao. Asymmetric cross-scale alignment for text-

- based person search. *IEEE Transactions on Multimedia*, 2022. 2, 6, 7
- [16] Li Jing, Pascal Vincent, Yann LeCun, and Yuan-dong Tian. Understanding dimensional collapse in contrastive self-supervised learning. *arXiv preprint arXiv:2110.09348*, 2021. 7
- [17] Minchul Kim, Anil K Jain, and Xiaoming Liu. Adaface: Quality adaptive margin for face recognition. In *Proceedings of the IEEE/CVF Conference on Computer Vision and Pattern Recognition (CVPR)*, pages 18750–18759, 2022. 3
- [18] Wonjae Kim, Bokyung Son, and Ildoo Kim. Vilt: Vision-and-language transformer without convolution or region supervision. In *International Conference on Machine Learning*, pages 5583–5594. PMLR, 2021. 3
- [19] Junnan Li, Ramprasaath Selvaraju, Akhilesh Gotmare, Shafiq Joty, Caiming Xiong, and Steven Chu Hong Hoi. Align before fuse: Vision and language representation learning with momentum distillation. *Advances in Neural Information Processing Systems*, 34:9694–9705, 2021. 2, 3
- [20] Shiping Li, Min Cao, and Min Zhang. Learning semantic-aligned feature representation for text-based person search. In *ICASSP 2022-2022 IEEE International Conference on Acoustics, Speech and Signal Processing (ICASSP)*, pages 2724–2728. IEEE, 2022. 2, 6
- [21] Shuang Li, Tong Xiao, Hongsheng Li, Bolei Zhou, Dayu Yue, and Xiaogang Wang. Person search with natural language description. In *Proceedings of the IEEE Conference on Computer Vision and Pattern Recognition (CVPR)*, pages 1970–1979, 2017. 1, 2, 5, 6
- [22] Deyin Liu, Lin Wu, Feng Zheng, Lingqiao Liu, and Meng Wang. Verbal-person nets: Pose-guided multi-granularity language-to-person generation. *IEEE Transactions on Neural Networks and Learning Systems*, 2022. 2, 6
- [23] Hao Liu, Xiangyu Zhu, Zhen Lei, and Stan Z Li. Adaptiveface: Adaptive margin and sampling for face recognition. In *Proceedings of the IEEE/CVF Conference on Computer Vision and Pattern Recognition (CVPR)*, pages 11947–11956, 2019. 3
- [24] Weiyang Liu, Yandong Wen, Zhiding Yu, and Meng Yang. Large-margin softmax loss for convolutional neural networks. *arXiv preprint arXiv:1612.02295*, 2016. 3
- [25] Hao Luo, Youzhi Gu, Xingyu Liao, Shenqi Lai, and Wei Jiang. Bag of tricks and a strong baseline for deep person re-identification. In *Proceedings of the IEEE/CVF Conference on Computer Vision and Pattern Recognition workshops*, pages 0–0, 2019. 1
- [26] Qiang Meng, Shichao Zhao, Zhida Huang, and Feng Zhou. Magface: A universal representation for face recognition and quality assessment. In *Proceedings of the IEEE/CVF Conference on Computer Vision and Pattern Recognition (CVPR)*, pages 14225–14234, 2021. 3
- [27] Alec Radford, Jong Wook Kim, Chris Hallacy, Aditya Ramesh, Gabriel Goh, Sandhini Agarwal, Girish Sastry, Amanda Askell, Pamela Mishkin, Jack Clark, et al. Learning transferable visual models from natural language supervision. In *International conference on machine learning*, pages 8748–8763. PMLR, 2021. 2
- [28] Alec Radford, Karthik Narasimhan, Tim Salimans, Ilya Sutskever, et al. Improving language understanding by generative pre-training. 2018. 3
- [29] Florian Schroff, Dmitry Kalenichenko, and James Philbin. Facenet: A unified embedding for face recognition and clustering. In *Proceedings of the IEEE Conference on Computer Vision and Pattern Recognition*, pages 815–823, 2015. 2
- [30] Xiujun Shu, Wei Wen, Haoqian Wu, Keyu Chen, Yiran Song, Ruizhi Qiao, Bo Ren, and Xiao Wang. See finer, see more: Implicit modality alignment for text-based person retrieval. In *Computer Vision—ECCV 2022 Workshops: Tel Aviv, Israel, October 23–27, 2022, Proceedings, Part V*, pages 624–641. Springer, 2023. 2, 7
- [31] Yifan Sun, Changmao Cheng, Yuhan Zhang, Chi Zhang, Liang Zheng, Zhongdao Wang, and Yichen Wei. Circle loss: A unified perspective of pair similarity optimization. In *Proceedings of the IEEE/CVF Conference on Computer Vision and Pattern Recognition (CVPR)*, pages 6398–6407, 2020. 3, 4
- [32] Ashish Vaswani, Noam Shazeer, Niki Parmar, Jakob Uszkoreit, Llion Jones, Aidan N Gomez, Łukasz Kaiser, and Illia Polosukhin. Attention is all you need. *Advances in neural information processing systems*, 30, 2017. 2, 5
- [33] Chengji Wang, Zhiming Luo, Yaojin Lin, and Shaozi Li. Text-based person search via multi-granularity embedding learning. In *The International Joint Conference on Artificial Intelligence (IJCAI)*, pages 1068–1074, 2021. 2, 6
- [34] Hao Wang, Yitong Wang, Zheng Zhou, Xing Ji, Dihong Gong, Jingchao Zhou, Zhifeng Li, and Wei Liu. Cosface: Large margin cosine loss for deep face recognition. In *Proceedings of the IEEE Conference on Computer Vision and Pattern Recognition (CVPR)*, pages 5265–5274, 2018. 3

- [35] Zhe Wang, Zhiyuan Fang, Jun Wang, and Yezhou Yang. Vitaa: Visual-textual attributes alignment in person search by natural language. In *Proceedings of the European Conference on Computer Vision (ECCV)*, pages 402–420. Springer, 2020. 2, 6, 7
- [36] Zijie Wang, Aichun Zhu, Jingyi Xue, Daihong Jiang, Chao Liu, Yifeng Li, and Fangqiang Hu. Sum: Serialized updating and matching for text-based person retrieval. *Knowledge-Based Systems*, 248:108891, 2022. 6, 7
- [37] Zijie Wang, Aichun Zhu, Jingyi Xue, Xili Wan, Chao Liu, Tian Wang, and Yifeng Li. Caibc: Capturing all-round information beyond color for text-based person retrieval. In *Proceedings of the 30th ACM International Conference on Multimedia*, pages 5314–5322, 2022. 6
- [38] Shuanglin Yan, Neng Dong, Liyan Zhang, and Jinhui Tang. Clip-driven fine-grained text-image person re-identification. *arXiv preprint arXiv:2210.10276*, 2022. 2, 3, 6, 7
- [39] Shuanglin Yan, Hao Tang, Liyan Zhang, and Jinhui Tang. Image-specific information suppression and implicit local alignment for text-based person search. *arXiv preprint arXiv:2208.14365*, 2022. 6, 7
- [40] Xiaohua Zhai, Xiao Wang, Basil Mustafa, Andreas Steiner, Daniel Keysers, Alexander Kolesnikov, and Lucas Beyer. Lit: Zero-shot transfer with locked-image text tuning. In *Proceedings of the IEEE/CVF Conference on Computer Vision and Pattern Recognition*, pages 18123–18133, 2022. 5
- [41] Pengchuan Zhang, Xiujun Li, Xiaowei Hu, Jianwei Yang, Lei Zhang, Lijuan Wang, Yejin Choi, and Jianfeng Gao. Vinvl: Revisiting visual representations in vision-language models. In *Proceedings of the IEEE/CVF Conference on Computer Vision and Pattern Recognition*, pages 5579–5588, 2021. 2
- [42] Ying Zhang and Huchuan Lu. Deep cross-modal projection learning for image-text matching. In *Proceedings of the European Conference on Computer Vision (ECCV)*, pages 686–701, 2018. 2, 4, 6, 7
- [43] Kecheng Zheng, Wu Liu, Jiawei Liu, Zheng-Jun Zha, and Tao Mei. Hierarchical gumbel attention network for text-based person search. In *Proceedings of the 28th ACM International Conference on Multimedia*, pages 3441–3449, 2020. 6
- [44] Zhedong Zheng, Liang Zheng, Michael Garrett, Yi Yang, Mingliang Xu, and Yi-Dong Shen. Dual-path convolutional image-text embeddings with instance loss. *ACM Transactions on Multimedia Computing, Communications, and Applications (TOMM)*, 16(2):1–23, 2020. 2, 6, 7
- [45] Aichun Zhu, Zijie Wang, Yifeng Li, Xili Wan, Jing Jin, Tian Wang, Fangqiang Hu, and Gang Hua. Dssl: Deep surroundings-person separation learning for text-based person retrieval. In *Proceedings of the 29th ACM International Conference on Multimedia*, pages 209–217, 2021. 2, 5, 6, 7